# Role of the receptor Mas in macrophage-mediated inflammation in vivo

Anna Hammer[a,1], Guang Yang[b,1], Juliane Friedrich[a], Agnes Kovacs[a], De-Hyung Lee[a], Katharina Grave[b], Stefanie Jörg[a], Natalia Alenina[c], Janina Grosch[d], Jürgen Winkler[d], Ralf Gold[e], Michael Bader[f,g,h,i,j], Arndt Manzel[a], Lars C. Rump[b], Dominik N. Müller[c,h], Ralf A. Linker[a,2,3], and Johannes Stegbauer[b,2,3]

[a]Department of Neurology, Friedrich-Alexander-University Erlangen-Nuremberg, 91054 Erlangen, Germany; [b]Department of Nephrology, Medical Faculty, Heinrich-Heine University Düsseldorf, 40225 Düsseldorf, Germany; [c]Max-Delbrück-Center for Molecular Medicine, 13125 Berlin, Germany; [d]Department of Molecular Neurology, Friedrich-Alexander-University Erlangen-Nuremberg, 91054 Erlangen, Germany; [e]Department of Neurology, Ruhr-University Bochum, 44801 Bochum, Germany; [f]Charité-University Medicine, 10117 Berlin, Germany; [g]German Center for Cardiovascular Research, Partner Site Berlin, 13347 Berlin, Germany; [h]Institute for Biology, University of Lübeck, 23538 Lübeck, Germany; [i]Experimental and Clinical Research Center, a joint cooperation of Max Delbrück Center for Molecular Medicine and Charité Medical Faculty, 13125 Berlin, Germany; and [j]Berlin Institute of Health, 10117 Berlin, Germany

Edited by Lawrence Steinman, Stanford University School of Medicine, Stanford, CA, and approved October 14, 2016 (received for review August 1, 2016)

**Recently, an alternative renin–angiotensin system pathway has been described, which involves binding of angiotensin-(1–7) to its receptor Mas. The Mas axis may counterbalance angiotensin-II–mediated proinflammatory effects, likely by affecting macrophage function. Here we investigate the role of Mas in murine models of autoimmune neuroinflammation and atherosclerosis, which both involve macrophage-driven pathomechanisms. Mas signaling affected macrophage polarization, migration, and macrophage-mediated T-cell activation. Mas deficiency exacerbated the course of experimental autoimmune encephalomyelitis and increased macrophage infiltration as well as proinflammatory gene expression in the spleen and spinal cord. Furthermore, Mas deficiency promoted atherosclerosis by affecting macrophage infiltration and migration and led to increased oxidative stress as well as impaired endothelial function in ApoE-deficient mice. In summary, we identified the Mas axis as an important factor in macrophage function during inflammation of the central nervous and vascular system in vivo. Modulating the Mas axis may constitute an interesting therapeutic target in multiple sclerosis and/or atherosclerosis.**

atherosclerosis | EAE | inflammation | macrophages | renin–angiotensin system

The renin–angiotensin system (RAS) with its active metabolite angiotensin (Ang) II is involved in the control of blood pressure, electrolyte balance, and sympathetic nerve activity and plays a major role in the pathogenesis of cardiovascular diseases (1, 2). Ang II mediates the majority of its effects via the Ang II type 1 (AT1) receptor. Blockade of the AT1 receptor reduces blood pressure and decelerates the progression of atherosclerosis. In addition to its well-defined hemodynamic effects, studies have indicated that AT1 receptor activation also contributes to target organ damage involving proinflammatory pathways. Thus, it has been shown that deletion of immune cells or immune suppression therapy reduces Ang II-dependent hypertension and hypertensive end organ damage, respectively (3, 4). In line with these results, recent studies have provided profound evidence that AT1 receptor inhibition directly affects immune cell function and thereby ameliorates the clinical course of experimental autoimmune encephalomyelitis (EAE) (5, 6) or systemic lupus erythematosus (7, 8).

Recently, growing evidence suggests that Ang II is not the only active peptide of the RAS. A particular example is the heptapeptide Ang-(1–7), which is derived from Ang I and Ang II by several metalloproteinases and endopeptidases including ACE2 and neprilysin. Ang-(1–7) has been shown to activate its own seven-transmembrane G protein-coupled receptor called Mas (9, 10). Mas is expressed on various tissues of the central nervous (CNS) and cardiovascular system (11). Recent studies have demonstrated that Ang-(1–7)-mediated Mas activation counter-regulates the pathophysiological effects of Ang II in the cardiovascular system (9, 12, 13). Accordingly, deletion of the receptor Mas resulted in blood pressure increase and endothelial dysfunction (14) whereas Ang-(1–7) infusion improved vascular function by inducing nitric oxide and prostaglandin release (15–17). Moreover, Ang-(1–7) has been shown to reduce reactive oxygen species production and vascular inflammation, thereby slowing down the progression of atherosclerosis in mice (18). Although many studies have indicated a clear role of the Ang-(1–7)/Mas axis in vascular inflammation, not much is known about the influence of Mas on immune cells and their function during inflammatory processes. However, Mas transcripts are up-regulated in macrophages after LPS exposure, and the Ang-(1–7) peptide drives an anti-inflammatory response in LPS-induced macrophages (19).

To investigate the role of the Ang-(1–7)/Mas axis on macrophages in vivo, we used two different animal models: EAE, a mouse model for multiple sclerosis (20), and hypercholesterinemic apolipoproteinE knockout (ApoEKO), a mouse model for human atherosclerosis (21).

## Results

**Mas Is Expressed on Different Macrophage Subtypes.** Protein and mRNA expression analysis showed that Mas is expressed on

### Significance

**The alternative renin–angiotensin system pathway, the angiotensin (Ang)-(1–7)/Mas axis, may counterbalance Ang II-mediated proinflammatory effects. To investigate the role of the Ang-(1–7)/Mas axis in immune cell function and inflammatory diseases in vivo, we used two different chronic inflammatory animal models. Deletion of Mas affects macrophage function and phenotype independently of the underlying phagocyte stimulus and aggravates the clinical course of experimental autoimmune encephalomyelitis as well as atherosclerosis in mice by tipping the in vivo balance from M(IL-4+IL-13)- to M(LPS+IFNγ)-like macrophages. Thus, modulation of the Ang-(1–7)/Mas axis counteracts the proinflammatory role of Ang II by regulating the delicate equilibrium between M(LPS+IFNγ)- and M(IL-4+IL-13)-like macrophages, thereby representing a promising pharmacological target for chronic inflammatory diseases.**

Author contributions: A.H., G.Y., D.-H.L., K.G., N.A., M.B., A.M., L.C.R., D.N.M., R.A.L., and J.S. designed research; A.H., G.Y., J.F., A.K., K.G., S.J., N.A., A.M., and J.S. performed research; J.G. and J.W. contributed new reagents/analytic tools; A.H., G.Y., J.F., A.K., K.G., S.J., N.A., A.M., and J.S. analyzed data; and A.H., R.G., R.A.L., and J.S. wrote the paper.

The authors declare no conflict of interest.

This article is a PNAS Direct Submission.

[1]A.H. and G.Y. contributed equally to this work.

[2]R.A.L. and J.S. contributed equally to this work.

[3]To whom correspondence may be addressed. Email: ralf.linker@uk-erlangen.de or johannes.stegbauer@med.uni-duesseldorf.de.

This article contains supporting information online at www.pnas.org/lookup/suppl/doi:10.1073/pnas.1612668113/-/DCSupplemental.

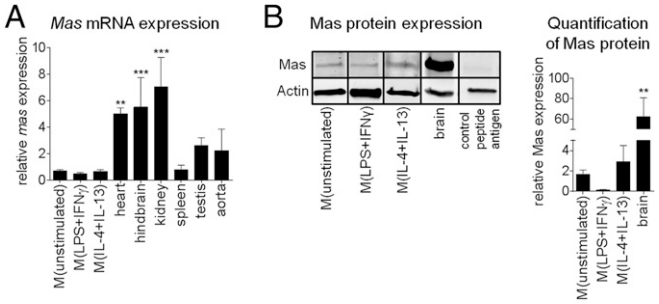


**Fig. 1.** Mas is expressed on different macrophage subsets. Mas expression is detectable on the mRNA (*A*) and protein (*B*) level in mature M(unstimulated) as well as M(LPS+IFNγ) and M(IL-4+IL-13) polarized BMDM. *Mas* expression in the spleen, testis, and aorta did not significantly differ compared with macrophages but was higher in the heart, kidney, and hindbrain (*A*). Data are presented as relative expression with the respective gene/protein expression in M(unstimulated) macrophages set to 1 [$n = 4$–5 per group for qRT-PCR and $n = 4$ for Western Blot analysis, mean ± SEM, $^{**}P < 0.01$, $^{***}P < 0.001$ compared with M(unstimulated)]. A receptor Mas control peptide antigen is used as negative control.

macrophages (Fig. 1 *A* and *B*). According to the nomenclature by Murray et al. (22), Mas was detected not only on unstimulated mature macrophages but also on M(LPS+IFNγ) and M(IL-4+IL-13) macrophages (Fig. 1 *A* and *B*). Compared with macrophages, *mas* expression did not significantly differ in the spleen, testis, and aorta (Fig. 1*A*). Only in the heart, kidney, and hindbrain, the most relevant brain region for neuroinflammation, was the expression of *mas* significantly higher than in macrophages (Fig. 1*A*). In contrast, *mas* expression in cultured hippocampal neurons, astrocytes, oligodendrocytes, and microglia was lower compared with macrophages (Fig. S1*A*). Furthermore, the expression of *mas* in the brain was rather inhomogeneous and restricted to specialized cell subsets and specific areas (Fig. S1*B*).

**Mas-Affected Macrophage Gene Expression, Migration, and T-Cell Activation Capacity.** Bone marrow-derived macrophages (BMDM) from Mas knockout (MasKO) and wild type (WT) mice were polarized in vitro into M(LPS+IFNγ) or M(IL-4+IL-13) macrophages. Macrophages derived from Mas-deficient mice showed significantly higher expression levels of M(LPS+IFNγ) markers, like *ccl2* and *tnfa*, compared with macrophages derived from WT mice (Fig. 2*A*). In contrast, the expression of the M(IL-4+IL-13) marker genes *ym1*, *fizz*, *mrc1*, and *mgl2* was strongly down-regulated in Mas-deficient macrophages compared with WT controls (Fig. 2*B*). Notably, pharmacological activation of Mas via its selective agonist AVE 0991 caused a significant reduction in the expression of M(LPS+IFNγ) profile genes but an increased M(IL-4+IL-13) marker gene expression (Fig. S2*A*). Furthermore, treatment with AVE 0991 reduced M(LPS+IFNγ) surface marker expression (CD80, CD86, and MHCII) but elevated the expression of CD206 on M(IL-4+IL-13) macrophages (Fig. S2*B*), indicating a shift toward M(IL-4+IL-13)–polarized macrophages after pharmacological Mas activation in vitro.

As shown in Fig. 2*C*, transmigration of macrophages isolated from MasKO mice was significantly increased compared with macrophages from WT mice.

In a following step, we investigated whether Mas on macrophages influences their capacity to activate naive T cells in vitro. Compared with WT macrophages, significantly more T cells proliferated when cocultured with Mas-deficient M(LPS+IFNγ) or M(IL-4+IL-13) macrophages (Fig. 2*D*), suggesting that the absence of the receptor Mas on macrophages rather than the phenotype of the macrophages influences T-cell proliferation. Additionally, treatment of M(IL-4+IL-13) but not M(LPS+IFNγ) macrophages with AVE 0991 before coculture with carboxyfluorescein succinimidyl ester-labeled naive T cells significantly reduced the number of proliferating T cells (Fig. S2*C*). Furthermore, mice treated with AVE 0991, starting 3 d before immunization, showed a significantly reduced disease incidence and a slightly ameliorated clinical EAE course (Fig. S2 *D* and *E*).

**Mas Deficiency Did Not Directly Affect T-Cell Differentiation and Proliferation in Vitro.** In T-cell monoculture, no differences in Th1 and Th17 differentiation were detected between the Mas deficient and the WT group (Fig. S3*A*). AVE 0991 (1 μM and 10 μM) also did not alter the differentiation from naive T cells to Th1 or Th17 cells (Fig. S3*B*). Furthermore, Mas deficiency did not influence T-cell proliferation rates (Fig. S3*C*).

**Mas Deficiency Exacerbated the Course of EAE and Increased Macrophage Infiltration, as Well as Th1 Frequencies.** Compared with naive mice, *mas* expression was decreased in the spleen during the acute phase of EAE [day 10 post immunization (p.i.)] but significantly increased in the spinal cord (Fig. 3 *A* and *B*). Interestingly, the expression pattern of *mas* in the spinal cord returned to baseline levels during the early chronic phase of the disease (day 28 p.i.) (Fig. 3 *A* and *B*). In active myelin oligodendrocyte glycoprotein (MOG)-EAE, Mas deficiency significantly aggravated the disease course (Fig. 3*C*) ($n = 7$; $^{**}P < 0.01$ on day 22 p.i.; one of two representative experiments is shown). Both groups showed a comparable disease incidence and no mortality. In a modified open field test, naive MasKO mice showed no alterations in locomotor activity and anxiety-like behavior compared with WT mice, suggesting similar baseline conditions for the analysis of EAE symptoms (Fig. S4 *A* and *B*).

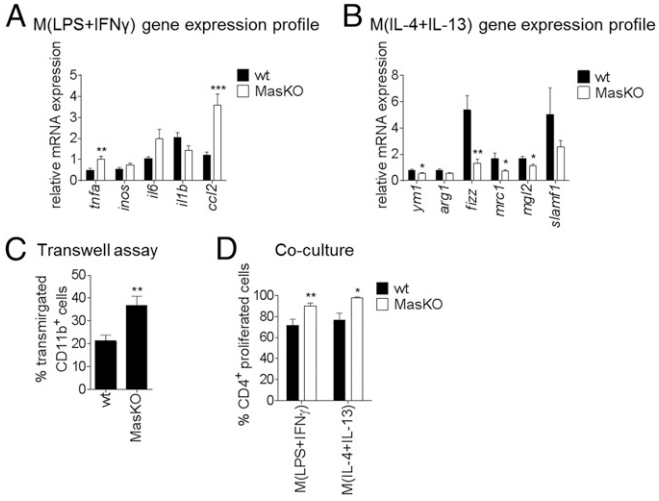


**Fig. 2.** Mas-deficient macrophages show an increase in proinflammatory M(LPS+IFNγ) but a decrease in anti-inflammatory M(IL-4+IL-13) marker gene expression, enhanced migration, and increased T-cell activation capacities. (*A*) Compared with WT mice, M(LPS+IFNγ) macrophages from MasKO mice display a significantly enhanced expression of the proinflammatory cytokines *ccl2* and *tnfa* and a trend toward higher levels of *il6* and *inos*. (*B*) A significant decrease in M(IL-4+IL-13) marker gene expression, for example, in *ym1*, *fizz*, *mrc1*, and *mgl2*, is detected in Mas-deficient macrophages compared with WT controls. Data are presented as relative expression of the indicated genes ($n = 4$–6 per group, mean ± SEM, $^{*}P < 0.05$, $^{**}P < 0.01$, $^{***}P < 0.001$). (*C*) The migration rate of Mas-deficient peritoneal macrophages is increased by around 20% compared with WT macrophages (data are pooled from a total of three independent experiments; $^{**}P < 0.01$, mean ± SEM). Data are compiled from an in vitro FCS-gradient Transwell assay. (*D*) Coculture assays of naive T cells with in vitro-generated BMDM display a significant increase in proliferating T cells when cultured with Mas-deficient M(LPS+IFNγ) and M(IL-4+IL-13) macrophages (data are pooled from a total of three independent experiments; $^{*}P < 0.05$, $^{**}P < 0.01$, mean ± SEM).

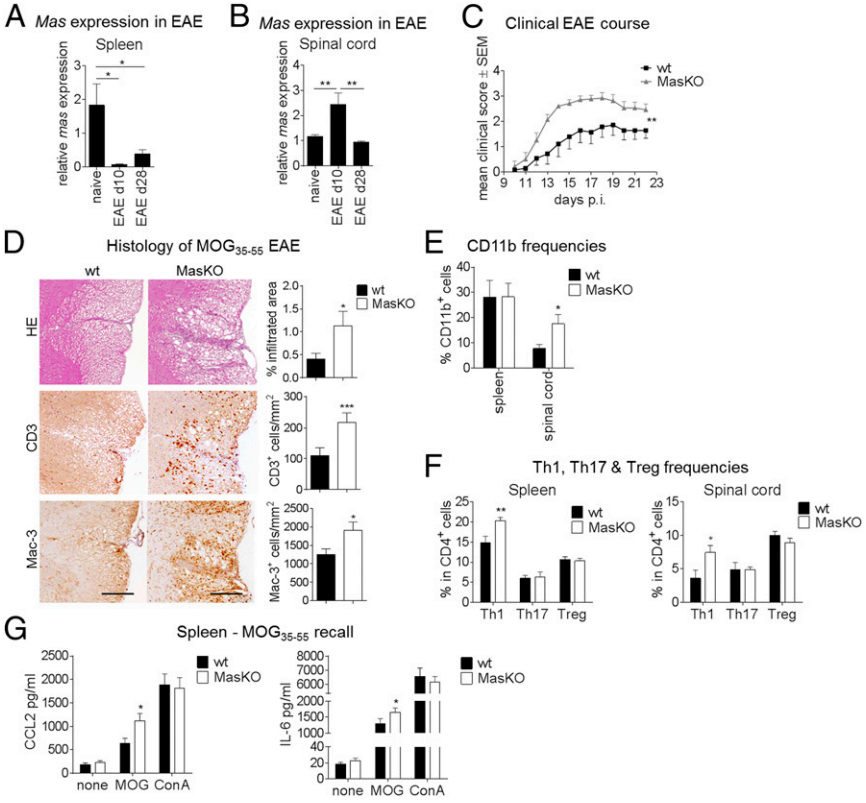


**Fig. 3.** Mas deficiency aggravates clinical symptoms of EAE and enhances macrophage infiltration and Th1 frequencies in the CNS. Active EAE is induced in C57BL/6 and MasKO mice. (*A* and *B*) Compared with healthy control mice, *mas* expression is significantly down-regulated in the spleen (*A*) but up-regulated in the spinal cord (*B*) during the acute phase of EAE (d10). In the early chronic phase (day 28 p.i.), expression of *mas* in the spinal cord (*B*) returns to baseline levels. (*C*) Mas deficiency significantly exacerbates the course of EAE ($n = 7$, $^{**}P < 0.01$ on day 22 p.i., mean ± SEM; one of two representative experiments is shown). (*D*) Mas deficiency leads to enlarged infiltrated areas and enhanced infiltration of Mac-3$^+$ macrophages/microglia and CD3$^+$ T cells on spinal cord cross-sections obtained at the maximum of disease. Representative images from the anterior columns of the thoracolumbar spinal cord are shown (Scale bar, 50 μm for all images.) (*E*) Ex vivo FACS phenotyping of the spleen and spinal cord infiltrates revealed that Mas deficiency increases CD11b$^+$ antigen-presenting cell frequencies in the CNS but not in the spleen on day 14 p.i. ($n = 7$–8, $^*P < 0.05$, mean ± SEM). (*F*) Ex vivo FACS analysis also shows enhanced Th1 frequencies in the spleen as well as spinal cord of MasKO mice on day 14 p.i. whereas Th17 and Treg cells remain unchanged ($n = 4$, $^*P < 0.05$, $^{**}P < 0.01$, $^{***}P < 0.001$, mean ± SEM). (*G*) Mas deficiency enhances CCL2 and IL-6 secretion after $MOG_{35–55}$-specific recall in total splenocytes on day 10 p.i. ($n = 8$, mean ± SEM).

Immunohistopathological analysis of the spinal cord (at day 22 p.i.) revealed increased CD3$^+$ T-cell and Mac-3$^+$ macrophage/microglia infiltration in MasKO mice compared with WT controls (Fig. 3*D*). Finally, Mas deficiency resulted in increased demyelination and loss of axons in inflamed lesions as well as augmented neuronal loss in the spinal cord compared with WT controls, which explains the more severe clinical course of MOG-EAE in Mas-deficient mice (Fig. S5 *A*–*C*).

Ex vivo phenotyping of the spleen and spinal cord of Mas-deficient mice during EAE showed increased CD11b$^+$ antigen-presenting cell frequencies in the CNS but not in the spleen ($n =$ 7–8) (Fig. 3*E*). Additionally, CD11b$^+$ cells in the spinal cord of MasKO mice displayed significantly reduced levels of the M(IL-4+IL-13) markers CD14 and CD206 but no significant difference in the expression of the M(LPS+IFNγ) markers CD80 and CD86 (Fig. S5*D*). We also found enhanced Th1 frequencies in the spleen as well as the spinal cord of MasKO mice compared with the WT group whereas the number of Th17 and Treg cells remained unchanged ($n = 4$) (Fig. 3*F*).

Finally, recall assays on day 10 p.i. revealed an enhanced secretion of the proinflammatory chemokines/cytokines CCL2 and IL-6 by Mas-deficient splenocytes compared with WT cells (Fig. 3*G*).

**Mas Knockout Enhanced Proinflammatory Gene Expression in the Spinal Cord and Spleen.** The proinflammatory macrophage genes *il6*, *il1b*, *tnfa*, *inos*, and *ccl2* were significantly higher expressed in the spinal cord of MOG-EAE–diseased MasKO mice compared with WT controls (Fig. 4*A*), whereas in the spleen only the expression of *il6*, *il1b*, and *ccl2* was enhanced (Fig. 4*C*). In contrast, the expression of some M(IL-4+IL-13)-like marker genes was decreased (e.g., *fizz*, *slamf1*) whereas the expression of others was increased in the spinal cord (Fig. 4*B*) as well as in the spleen (Fig. 4*D*) of Mas-deficient animals compared with WT controls.

**Mas Deficiency Leads to Increased Oxidative Stress and Impaired Endothelial Function in ApoEKO Mice.** In ApoEKO mice, Mas deficiency led to increased endothelial dysfunction, a known risk factor for atherosclerosis (Fig. 5*A*). To understand the underlying mechanism for impaired vascular function in Mas-deficient ApoEKO mice, we measured reactive oxidative stress in ApoEKO and ApoEKO/MasKO mice. Urinary 8-isoprostane and aortic nitrotyrosine expression levels were increased in ApoEKO/MasKO mice (Fig. 5 *B* and *C*).

**Mas Deficiency Exaggerated Atherosclerosis by Affecting Macrophage Infiltration, Migration, and Cytokine Expression.** As shown in Fig. 6 *A* and *B*, Mas deficiency leads to a significant exaggeration of atherosclerosis in the aortic arch region of ApoEKO mice. Mas deficiency led to enhanced macrophage infiltration within the atherosclerotic plaques of the aortic root (Fig. 6*C*). Moreover, the propensity to migrate was significantly increased in macrophages from ApoEKO/MasKO mice compared with ApoEKO mice, suggesting an important role of Mas in macrophage function in ApoEKO mice (Fig. 6*D*). Mas deficiency was associated with proinflammatory macrophage cytokine expression, such as *il-6*, *inos*, *ccl2* and *il12p40*, in atherosclerotic aortas of ApoEKO mice (Fig. 6*E*). Cytokine levels in the plasma (Fig. S6*A*) were not significantly affected by Mas. Moreover, Mas deficiency did not influence the frequency of CD11c$^+$, CD11b$^+$, CD3$^+$, CD4$^+$, and CD8$^+$ cells measured in the spleen of ApoEKO mice (Fig. S6*B*).

## Discussion

Here we investigate potential effects of the Ang-(1–7)/Mas axis on macrophage function using MOG-EAE mice as a model of multiple sclerosis and hypercholesterinemic ApoEKO mice as a model of atherosclerosis. Both animal models are characterized by macrophage-mediated inflammation. In the present study, we show that Mas deficiency affects macrophage phenotypes and function, thereby aggravating the disease course in both settings. At first glance, an autoimmune disease model like MOG-EAE

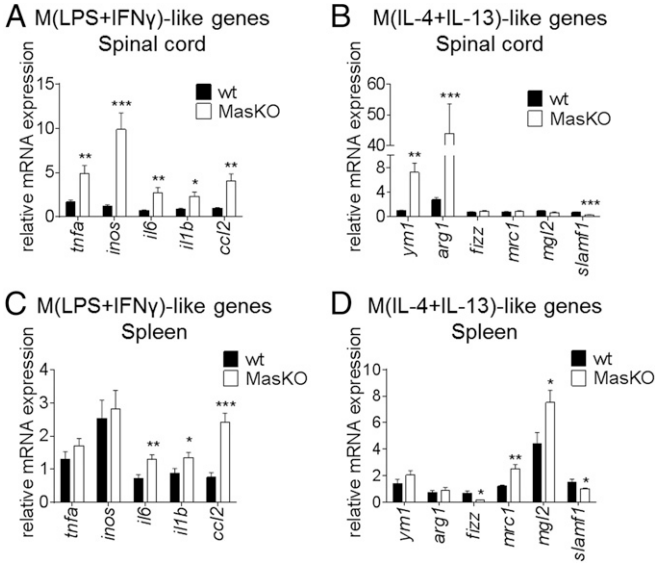


**Fig. 4.** Mas knockout increases proinflammatory gene expression in the spinal cord and spleen. mRNA expression in the spinal cord (*A* and *B*) and spleen (*C* and *D*) was analyzed by qRT-PCR on day 22 p.i.. Mas deficiency increases the expression level of the proinflammatory M(LPS+IFNγ)-like macrophage markers *il6*, *il1b*, *tnfa*, *inos*, and *ccl2* in the spinal cord (*A*) and spleen (*C*) of EAE mice by up to 10-fold. The expression of some M(IL-4+IL-13)-like marker genes is also altered in the spinal cord (*B*) and spleen (*D*) of MasKO mice compared with the WT controls ($n = 4$, $*P < 0.05$, $**P < 0.01$, $***P < 0.001$, mean ± SEM).

and a cardiovascular disease model like atherosclerosis may not have much in common. However, our data strikingly show that disruption of the alternative renin–angiotensin system pathway at the receptor level similarly affects macrophage function and phenotype independently of the underlying phagocyte stimulus.

Specifically, deletion of the receptor Mas enhances the migratory capacity and induces a proinflammatory phenotype of macrophages in MOG-EAE as well as ApoEKO mice, leading to an increased immune cell infiltration in the spinal cord or in atherosclerotic plaques, respectively. Previously, several studies have shown that deletion of ACE2, one of the key enzymes in Ang II degradation and a member of the alternative RAS pathway with its ACE2/Ang-(1–7)/Mas axis, results in increased vascular inflammation leading to a progression of atherosclerosis (23). However, as ACE2 deficiency also leads to an accumulation of the proinflammatory metabolite Ang II, the role of the alternative pathway in the regulation of these effects was unclear. Here, we definitely show that the Ang-(1–7)/Mas axis influences the inflammatory capacity of immune cells in two different, yet distinct, chronic inflammatory diseases.

Moreover, we specify the immune cell subset with a prevailing role of Mas. Although Mas is expressed on different cell types, Mas deficiency particularly affects $CD11b^+$ macrophages in vitro and in vivo by interfering with cytokine expression and activation capacities of different macrophage subtypes. Well in line with our in vitro data, previous studies on the Ang-(1–7)/Mas axis in peritoneal macrophages also implied a role of Mas in cell migration. Additionally, enhanced T-cell proliferation in in vitro coculture experiments with Mas-deficient macrophages may be explained by a lack of inhibitory Ang-(1–7) signaling, which is known to suppress T-cell proliferation (24–26). This effect may be governed by a role of endogenous Mas in inhibiting M(LPS+IFNγ)-like polarization and proinflammatory cytokine expression. Previous work by Souza et al. (19) showed that Mas-signaling pathways rather exert anti-inflammatory effects: Treatment with Ang-(1–7) led to decreased *il6* and *tnfa* mRNA levels in peritoneal macrophages. Here, we extend these observations to in vivo models of macrophage dysfunction and show consistent data: Mas deficiency may drive proinflammatory M(LPS+IFNγ)-like responses and play a role in diminishing anti-inflammatory M(IL-4+IL-13)-like polarization in our animal models, in which the progression of the diseases is significantly characterized by macrophage-mediated inflammation.

In EAE, Mas deficiency enhances the frequency of macrophages in the spinal cord, the presence of which in the CNS is crucial for the local activation of infiltrating T cells and, thus, the initiation and progression of the disease (27). The enhanced Th1 frequencies found in the spinal cord of diseased Mas-deficient mice may be a downstream consequence of the increased $CD11b^+$ cell infiltration because these macrophages actually produce higher levels of chemoattractants, allowing T cells to cross the blood–brain barrier (BBB).

In models of cardiovascular diseases, such as atherosclerosis, an influence of the Ang-(1–7)/Mas axis on migration of $CD11b^+$ monocytes has already been shown. Here, chemokines and their receptors, such as CCL2 and CCR5, may play a crucial role (28, 29). Therefore, the increase of antigen-presenting cell migration into atherosclerotic plaques as well as the enhanced plaque size, which we observed in our ApoEKO mouse model, may be mediated by an effect of Mas on chemokine expression. Well in line with this observation, Mas deficiency enhances the expression of the chemokine CCL2 in vitro and in vivo with NF-κB as a key regulator (30, 31).

In summary, our data support the concept of the Ang-(1–7)/Mas axis as anti-inflammatory pathway in different macrophage-mediated disease models in vivo. Signaling via Mas modulates the delicate balance between M(LPS+IFNγ)-like and M(IL-4+IL-13)-like macrophages, pushing it toward the M(IL-4+IL-13)-like phenotype, which is an important regulator controlling inflammation and autoimmunity (32, 33). Therefore, the receptor Mas may be an interesting therapeutic target to treat autoimmune diseases via regulating inflammatory processes. A specific activation of Mas, e.g., via agonists like AVE 0991, may impair macrophage migration through the BBB or in the vessel wall, thus limiting inflammation in the CNS or the vascular system (28, 34, 35).

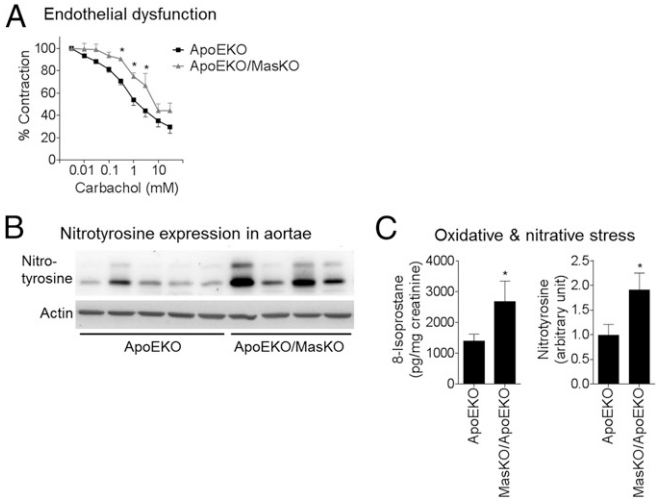


**Fig. 5.** Mas deficiency in ApoEKO mice increases oxidative stress and endothelial dysfunction. (*A*) Carbachol-induced vascular relaxation is significantly impaired in kidneys of ApoEKO/MasKO mice compared with ApoEKO mice ($n = 5$–10 per group). (*B* and *C*) In ApoEKO mice, Mas deficiency leads to increased oxidative stress measured by urinary 8-isoprostane and aortic nitrotyrosine expression levels (measurements were repeated for a total of three times; $n = 6$–8, $*P < 0.05$, mean ± SEM).

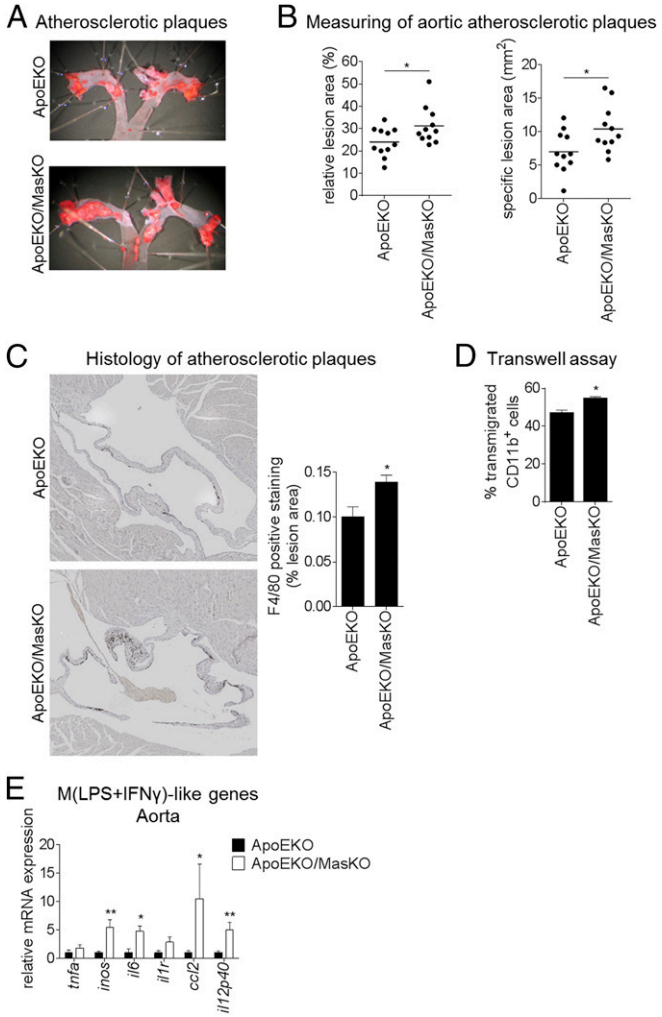


**Fig. 6.** Increased atherosclerotic plaque size, macrophage infiltration, and proinflammatory cytokine expression in ApoEKO/MasKO mice. (*A*) Mas deficiency leads to a significant exaggeration of atherosclerosis in the aortic arch region of ApoEKO mice. (*B*) The relative and the specific area of atherosclerotic lesions in the aorta are significantly enlarged in Mas-deficient ApoEKO mice ($n = 11$, $^*P < 0.05$). (*C*) Mas deficiency causes enhanced infiltration of F4/80$^+$ macrophages within the atherosclerotic plaques of the aortic root ($n = 6$, $^*P < 0.05$, mean ± SEM). (*D*) The migration rate of Mas-deficient peritoneal macrophages from ApoEKO mice, measured with an in vitro FCS-gradient Transwell assay, is significantly increased compared with ApoEKO mice (two independent experiments, each comprising two mice; $^*P < 0.05$, mean ± SEM). (*E*) Mas deficiency induces proinflammatory M(LPS+IFNγ)-like cytokines, such as *il6*, *inos*, *ccl2*, and *il12p40*, in atherosclerotic aortas of ApoEKO mice ($n = 6$, $^*P < 0.05$, $^{**}P < 0.01$, mean ± SEM).

## Materials and Methods

**Mice.** WT, MasKO (36), ApoEKO ,and ApoEKO/MasKO mice were backcrossed on a C57BL/6 background at least 10 times. All mice were obtained from an in-house breed at the local animal care facility of the University of Erlangen, the Max Delbrück Center for Molecular Medicine Berlin, or the University of Düsseldorf. All experiments were performed in accordance with the German laws for animal protection and were approved by both ethics committees of the University of Erlangen and University of Düsseldorf (AZ 54–2532.1–56/12 and AZ 84–02.04.2012.A250).

**EAE Induction.** Induction of active EAE was performed as previously described (37). Briefly, mice received a total of 200 μg $MOG_{35–55}$, 200 μg complete Freund's adjuvant (CFA), containing 4 mg/mL *Mycobacterium tuberculosis* (H37RA, BD Biosciences), and 200 ng pertussis toxin (List Biological Laboratories). AVE 0991 (0.06 mg/d/mouse in a 1% hydroxyethyl cellulose solution; Hycultec) was administered orally on a daily basis starting 3 d before immunization.

**Induction of Atherosclerosis.** Six-week-old ApoEKO and ApoEKO/MasKO mice were fed a high-fat "Western diet" (Sniff) (42% fat, 0.15% cholesterol) for 12 wk.

**Modified Open Field Test.** Eight to 10-wk-old WT and MasKO mice were placed in an empty arena for 20 min. The number of rearings and the time spent in the center as well as in the periphery were measured by a blinded observer.

**Immunohistochemistry and Tissue Staining.** Luxol Fast Blue staining was performed for evaluation of demyelination, Bielschowksy silver impregnation for axonal integrity/damage, and Nissl staining for motor neuron quantification. Hematoxylin and eosin (HE) staining was used to analyze the extent of infiltrated areas. Immunohistochemistry was performed on 5-μm-thick paraffin sections (αCD3 1:500, Bio-Rad; αMac-3 1:500, BD Pharmingen). For detailed quantification procedures, see *SI Materials and Methods*.

**Isolation of Peritoneal Macrophages.** The peritoneal cavity served as a primary source of naive macrophages. Ten milliliters of cold Dulbecco's phosphate-buffered saline (DPBS) was injected intraperitoneally two times. Typically, $2.5 \times 10^6$ cavity cells were isolated per mouse.

**Generation of BMDM.** Bone marrow cells were obtained from tibias and femurs of 10- to 20-wk-old C57BL/6 mice as described previously (38) and maintained in macrophage medium [RPMI-1640 + 10% (vol/vol) FCS + 1% penicillin/streptomycin + 1% L-glutamine] containing 10 ng/mL recombinant mouse M-CSF (Biolegend) for 8 d. Purity of BMDM (>97%) was determined as F4/80$^+$/CD11b$^+$ cells by flow cytometry (FACSCanto II, BD Biosciences). For analysis of pharmacological Mas activation, 0.1 μM AVE 0991 (Hycultec) was added to the cell culture medium.

**Macrophage Polarization.** After 8 d, BMDM were cultured for 2 additional days under polarizing conditions as follows: M(unstimulated), no cytokines; M(LPS+IFNγ), 100 ng/mL LPS + 10 ng/mL IFN-γ; M(IL-4+IL-13), 20 ng/mL IL-4 + 20 ng/mL IL-13 (recombinant cytokines were obtained from Biolegend).

**Isolation of Naive T Cells.** Splenic T cells were isolated by magnetic-activated cell sorting using the pan T-cell isolation kit II according to the manufacturer's instructions (Miltenyi Biotech). Cells were fluorescently stained with an antibody mixture containing αCD4-FITC (RM4-5, eBioscience), αCD44-PE (IM7, Biolegend), αCD62L-APC (MEL-14, eBioscience), and αCD25-PE-Cy5 (PC61.5, eBioscience) and were subsequently isolated by fluorescence-activated cell sorting on MoFlo (Beckman-Coulter) in the FACS-core unit in Erlangen. To monitor proliferation, cells were labeled with fixable Cell Proliferation Dye eFluor450 (eBioscience) according to the manufacturer's protocol.

**T-Cell Differentiation.** Sorted naive T cells (CD4$^+$CD62L$^+$CD44$^{low}$CD25$^-$) were stimulated by plate-bound anti-CD3 (2 μg/mL, 145–2C11, BD Pharmingen) and soluble anti-CD28 (2 μg/mL, 37.51, BD Pharmingen) and cultured for 4 d in the presence of IL-6 (40 ng/mL, R&D Systems) and TGFβ1 (1 ng/mL, Biolegend) for Th17 or IL-12p70 (20 ng/mL, R&D Systems) and anti–IL-4 (10 mg/mL, Biolegend) for Th1 differentiation. To determine the influence of the Mas selective agonist AVE 0991 on T-cell differentiation, cells were cultured with 1 μM or 10 μM AVE 0991 (Hycultec) for 4 d.

**Coculture Assay.** To induce proliferation, naive T cells were cultured in the presence of plate-bound αCD3 (2 μg/mL, 145–2C11, BD Pharmingen), soluble αCD28 (2 μg/mL, 37.51, BD Pharmingen), and polarized BMDM. Macrophages were seeded with naive T cells in a ratio of 1:6. After 4 d of differentiation, cells were harvested and analyzed by flow cytometry (FACSCantoII, BD Biosciences).

**Migration Assay.** Migration of macrophages was measured in a modified Boyden chamber assay using Transwell inserts with a 5-μm porous bottom (Corning Life Sciences). Peritoneal macrophages were loaded onto the migration chamber in macrophage medium containing 0.5% FCS. The lower chamber was loaded with macrophage medium containing 10% (vol/vol) FCS. After 18 h of migration, cells were stained for CD11b and quantified by flow cytometry (FACSCantoII, BD Biosiences).

**FACS Analysis.** For staining procedures, see *SI Materials and Methods*.

**In Vitro MOG Restimulation Assay.** Splenocytes from EAE mice were obtained on days 10–14 p.i. and seeded at a density of $3 \times 10^6$ cells/mL; $MOG_{35-55}$ (20 μg/mL) and Con A (1.25 μg/mL) were added for stimulation, and cells were cultured for 12–48 h. Cytokines in the supernatant were measured using precast ELISAs (R&D Systems). To monitor proliferation, cells were labeled with fixable Cell Proliferation Dye eFluor450 (eBioscience) according to the manufacturer's protocol.

**Real-Time PCR.** Total RNA was isolated and reversely transcribed using the RNeasy Kit (Qiagen) and the QuantiTect Reverse Transcription Kit (Qiagen). PCR reactions were performed at a 5-μL scale with a qTower real-time PCR System (Analytik Jena). Relative quantification was performed by the ΔΔCT method, normalizing target gene expression on *actb*/β-Actin or *gapdh* as housekeeping genes. For more details, see *SI Materials and Methods*.

**Western Blotting.** For detailed information about protein extraction and Western blotting, see *SI Materials and Methods*. Mas protein was detected by a rabbit anti–Ang-(1–7) Mas receptor antibody (1:250, #AAR-013, Alomone Laboratories). Mouse anti–β-Actin (1:1,000) was obtained from Abcam (ab8226). For blotting of aortic nitrotyrosine, primary polyclonal rabbit anti-Nitrotyrosine (1:1,000, ab94883, Abcam) and rabbit anti–β-Actin (1:6,000, # A5316, Sigma-Aldrich) antibodies were used.

**Isolated Perfused Kidney.** Endothelial dependent vasorelaxation was tested with the model of isolated perfused kidneys as described previously (39). In preconstricted renal vessels (norepinephrine, 1 μM), endothelial-dependent vasorelaxation was induced by carbachol (Sigma-Aldrich) in the presence of diclofenac (3 μM) and expressed as the percentage pressor response of the preconstricted kidney, which was set as 100%.

**Measurement of Urinary 8-Isoprostane.** Twelve weeks after the Western diet treatment, the urinary excretion rate of 8-isoprostane was measured using a colorimetric-assay kit (Cayman Chemical Company) and normalized to urinary creatinine concentration (50070, Cayman Chemical Company).

**Quantification of Atherosclerosis and Macrophage Infiltration.** The adventitia were removed from the aortic arch and stained with red oil O. Atherosclerotic lesions were quantified by using ImageJ (ImageJ 1.37v software, NIH). Macrophage accumulation was assessed with a rat anti-mouse antibody against F4/80 (Serotec; MCA497RT, clone C1:A3-1; 1:1,000). For more details, see *SI Materials and Methods*.

**Detection of Plasma Cytokines.** A commercially available luminex bead-based immunoassay (Bio-Plex Pro Mouse Cytokine 23-plex Assay #M60009RDPD, Bio-Rad) was used to determine plasma levels of IL-1β, IL-6, CCL2, RANTES, and TNF-α. Analysis was performed with a Bioplex 200 suspension array system (Bio-Rad) according to the manufacturer's instructions.

**Statistical Analysis.** Statistical testing was performed using GraphPad Prism (GraphPad Software Inc.). All in vitro and ex vivo data were analyzed by either one/two-way ANOVA followed by Tukey's posttest, unpaired *t* test, or Mann–Whitney *U* test after checking for normal distribution (unless otherwise indicated). EAE data were analyzed by Mann–Whitney *U* test for disease course and by log-rank test for disease incidence. Data are presented as mean ± SEM; $*P < 0.05$, $**P < 0.01$, or $***P < 0.001$ were considered to be statistically significant.

**ACKNOWLEDGMENTS.** We thank Silvia Seubert, Katrin Bitterer, and Christina Schwandt for expert technical assistance. J.S., G.Y., and L.C.R. were supported by the Deutsche Forschungsgemeinschaft (Grant IRTG1902). R.A.L. holds an endowed professorship supported by Novartis Pharma.

1. Burnier M, Brunner HR (2000) Angiotensin II receptor antagonists. *Lancet* 355(9204): 637–645.
2. Kim S, Iwao H (2000) Molecular and cellular mechanisms of angiotensin II-mediated cardiovascular and renal diseases. *Pharmacol Rev* 52(1):11–34.
3. Guzik TJ, et al. (2007) Role of the T cell in the genesis of angiotensin II induced hypertension and vascular dysfunction. *J Exp Med* 204(10):2449–2460.
4. Muller DN, et al. (2002) Immunosuppressive treatment protects against angiotensin II-induced renal damage. *Am J Pathol* 161(5):1679–1693.
5. Platten M, et al. (2009) Blocking angiotensin-converting enzyme induces potent regulatory T cells and modulates TH1- and TH17-mediated autoimmunity. *Proc Natl Acad Sci USA* 106(35):14948–14953.
6. Stegbauer J, et al. (2009) Role of the renin-angiotensin system in autoimmune inflammation of the central nervous system. *Proc Natl Acad Sci USA* 106(35): 14942–14947.
7. Esteban V, et al. (2003) Effect of simultaneous blockade of AT1 and AT2 receptors on the NFkappaB pathway and renal inflammatory response. *Kidney Int* 64(Suppl 86): S33–S38.
8. Mii A, et al. (2009) Angiotensin II receptor blockade inhibits acute glomerular injuries with the alteration of receptor expression. *Lab Invest* 89(2):164–177.
9. Kostenis E, et al. (2005) G-protein-coupled receptor Mas is a physiological antagonist of the angiotensin II type 1 receptor. *Circulation* 111(14):1806–1813.
10. Santos RAS, et al. (2003) Angiotensin-(1-7) is an endogenous ligand for the G protein-coupled receptor Mas. *Proc Natl Acad Sci USA* 100(14):8258–8263.
11. Metzger R, et al. (1995) Expression of the mouse and rat mas proto-oncogene in the brain and peripheral tissues. *FEBS Lett* 357(1):27–32.
12. Jiang F, et al. (2014) Angiotensin-converting enzyme 2 and angiotensin 1-7: Novel therapeutic targets. *Nat Rev Cardiol* 11(7):413–426.
13. Santos RA (2014) Angiotensin-(1-7). *Hypertension* 63(6):1138–1147.
14. Xu P, et al. (2008) Endothelial dysfunction and elevated blood pressure in MAS gene-deleted mice. *Hypertension* 51(2):574–580.
15. Brosnihan KB, Li P, Ferrario CM (1996) Angiotensin-(1-7) dilates canine coronary arteries through kinins and nitric oxide. *Hypertension* 27(3 Pt 2):523–528.
16. Sampaio WO, et al. (2007) Angiotensin-(1-7) through receptor Mas mediates endothelial nitric oxide synthase activation via Akt-dependent pathways. *Hypertension* 49(1):185–192.
17. Potthoff SA, et al. (2014) Angiotensin-(1-7) modulates renal vascular resistance through inhibition of p38 mitogen-activated protein kinase in apolipoprotein E-deficient mice. *Hypertension* 63(2):265–272.
18. Stegbauer J, et al. (2011) Chronic treatment with angiotensin-(1-7) improves renal endothelial dysfunction in apolipoproteinE-deficient mice. *Br J Pharmacol* 163(5): 974–983.
19. Souza LL, Costa-Neto CM (2012) Angiotensin-(1-7) decreases LPS-induced inflammatory response in macrophages. *J Cell Physiol* 227(5):2117–2122.
20. Herrero-Herranz E, Pardo LA, Gold R, Linker RA (2008) Pattern of axonal injury in murine myelin oligodendrocyte glycoprotein induced experimental autoimmune encephalomyelitis: Implications for multiple sclerosis. *Neurobiol Dis* 30(2):162–173.
21. Wassmann S, et al. (2004) Inhibition of diet-induced atherosclerosis and endothelial dysfunction in apolipoprotein E/angiotensin II type 1A receptor double-knockout mice. *Circulation* 110(19):3062–3067.
22. Murray PJ, et al. (2014) Macrophage activation and polarization: Nomenclature and experimental guidelines. *Immunity* 41(1):14–20.
23. Thomas MC, et al. (2010) Genetic Ace2 deficiency accentuates vascular inflammation and atherosclerosis in the ApoE knockout mouse. *Circ Res* 107(7):888–897.
24. Gallagher PE, Tallant EA (2004) Inhibition of human lung cancer cell growth by angiotensin-(1-7). *Carcinogenesis* 25(11):2045–2052.
25. Strawn WB, Ferrario CM, Tallant EA (1999) Angiotensin-(1-7) reduces smooth muscle growth after vascular injury. *Hypertension* 33(1 Pt 2):207–211.
26. Tallant EA, Ferrario CM, Gallagher PE (2005) Angiotensin-(1-7) inhibits growth of cardiac myocytes through activation of the mas receptor. *Am J Physiol Heart Circ Physiol* 289(4):H1560–H1566.
27. McMahon EJ, Bailey SL, Castenada CV, Waldner H, Miller SD (2005) Epitope spreading initiates in the CNS in two mouse models of multiple sclerosis. *Nat Med* 11(3):335–339.
28. Combadière C, et al. (2008) Combined inhibition of CCL2, CX3CR1, and CCR5 abrogates Ly6C(hi) and Ly6C(lo) monocytosis and almost abolishes atherosclerosis in hypercholesterolemic mice. *Circulation* 117(13):1649–1657.
29. Tacke F, et al. (2007) Monocyte subsets differentially employ CCR2, CCR5, and CX3CR1 to accumulate within atherosclerotic plaques. *J Clin Invest* 117(1):185–194.
30. El-Hashim AZ, et al. (2012) Angiotensin-(1-7) inhibits allergic inflammation, via the MAS1 receptor, through suppression of ERK1/2- and NF-κB-dependent pathways. *Br J Pharmacol* 166(6):1964–1976.
31. Ueda A, Ishigatsubo Y, Okubo T, Yoshimura T (1997) Transcriptional regulation of the human monocyte chemoattractant protein-1 gene. Cooperation of two NF-kappaB sites and NF-kappaB/Rel subunit specificity. *J Biol Chem* 272(49):31092–31099.
32. Cassetta L, Cassol E, Poli G (2011) Macrophage polarization in health and disease. *ScientificWorldJournal* 11:2391–2402.
33. Liu Y-C, Zou X-B, Chai Y-F, Yao Y-M (2014) Macrophage polarization in inflammatory diseases. *Int J Biol Sci* 10(5):520–529.
34. Moreno M, et al. (2014) Conditional ablation of astroglial CCL2 suppresses CNS accumulation of M1 macrophages and preserves axons in mice with MOG peptide EAE. *J Neurosci* 34(24):8175–8185.
35. Smith JD, et al. (1995) Decreased atherosclerosis in mice deficient in both macrophage colony-stimulating factor (op) and apolipoprotein E. *Proc Natl Acad Sci USA* 92(18): 8264–8268.
36. Walther T, et al. (1998) Sustained long term potentiation and anxiety in mice lacking the Mas protooncogene. *J Biol Chem* 273(19):11867–11873.
37. Haghikia A, et al. (2015) Dietary fatty acids directly impact central nervous system autoimmunity via the small intestine. *Immunity* 43(4):817–829.
38. Muccioli M, Pate M, Omosebi O, Benencia F (2011) Generation and labeling of murine bone marrow-derived dendritic cells with Qdot nanocrystals for tracking studies. *J Vis Exp* (52):e2785.
39. Stegbauer J, Oberhauser V, Vonend O, Rump LC (2004) Angiotensin-(1-7) modulates vascular resistance and sympathetic neurotransmission in kidneys of spontaneously hypertensive rats. *Cardiovasc Res* 61(2):352–359.